



# The influences of poly (ethylene glycol) chain length on hydrophilicity, oxygen permeability, and mechanical properties of multicomponent silicone hydrogels

Xueqin Zhang<sup>1</sup> · Lu Wang<sup>1</sup> · Huiwen Tao<sup>1</sup> · Ying Sun<sup>1</sup> · Hong Yang<sup>1</sup> · Baoping Lin<sup>1</sup>

Received: 31 January 2019 / Revised: 16 June 2019 / Accepted: 15 July 2019 / Published online: 25 July 2019  
© Springer-Verlag GmbH Germany, part of Springer Nature 2019

## Abstract

Two series of multicomponent silicone hydrogels based on poly (ethylene glycol)- polydimethylsiloxane-poly (ethylene glycol) (PEG-PDMS-PEG) triblock oligomers were prepared by copolymerization of silicon-containing monomers methacrylate-terminated PEG-PDMS-PEG (MTSM), tris (trimethylsiloxy)-3-methacryloxypropylsilane (TRIS), and hydrophilic monomers such as N,N-dimethylacrylamide (DMA), N-vinylpyrrolidone (NVP), and hydroxypropyl-methacrylate (HPMA). The influences of PEG chain length on hydrophilicity, oxygen permeability, and mechanical properties of silicone hydrogels were explored. The hydrophilic properties of silicone hydrogels were characterized by water contact angle, equilibrium water content, and swelling-dehydration process. The results showed that the water contact angles of dry samples decreased while the swollen ones increased with the increase of PEG chain length. The equilibrium water content decreased first and then increased as the length of the PEG chain increased. The results of swelling and dehydration process showed that PEG chains improved the water-retaining capacity of silicone hydrogels. Moreover, the protein adsorption of samples with PEG chains decreased. The surface morphologies of silicone hydrogels were characterized by scanning electron microscope (SEM), and a reconstruction model was proposed. In addition, the oxygen permeability and mechanical properties of silicone hydrogels also varied with the length of the PEG chain. These results could provide a theoretical reference for the design and modification of new hydrogels.

**Keywords** Silicone hydrogels · PEG chains · Hydrophilicity · Oxygen permeability · Mechanical properties

## Introduction

Silicone hydrogels are hydrogels that contain silicone polymer segments [1], and usually obtained by copolymerization of silicon-containing monomers with hydrophilic monomers such as N-vinylpyrrolidone (NVP) [2]. Compared with traditional hydrogels, the major advantages of silicone hydrogels are their excellent gas permeability, impressive mechanical property, and good biocompatibility. Silicone hydrogels have

been used extensively as biomedical materials, such as contact lenses [3, 4], histological engineering materials [5, 6], and drug-delivery carriers [7, 8].

Polydimethylsiloxane (PDMS), a kind of silicone rubber material, is widely used to prepare silicone hydrogels due to its good oxygen permeability, elasticity, and biocompatibility [9]. However, PDMS is hydrophobic and has low surface energy. The siloxane groups tend to accumulate on the surface of materials in copolymers, which leads to the hydrophobic surface of silicone hydrogels [10–12]. The hydrophobicity of silicone hydrogels limits their application in many fields, especially those where the hydrophilicity is a primary index. For example, the patients may feel uncomfortable due to the low hydrophilicity of contact lenses which are made from silicone hydrogels, and proteins may be adsorbed on the surface of biomaterials to form thrombosis.

Currently, many studies have focused on how to ameliorate the hydrophobicity of PDMS and followed by the improvement of the hydrophilicity of silicone hydrogels. Surface plasma treatment is one of the commonly used methods, which

**Electronic supplementary material** The online version of this article (<https://doi.org/10.1007/s00396-019-04544-z>) contains supplementary material, which is available to authorized users.

✉ Xueqin Zhang  
xqzhang@seu.edu.cn

✉ Baoping Lin  
lbp@seu.edu.cn

<sup>1</sup> School of Chemistry and Chemical Engineering, Southeast University, Nanjing 211189, People's Republic of China

can introduce hydroxyl and other hydrophilic groups on the surface of hydrogels to improve their hydrophilicity [13]. However, the diffusion of the unreacted oligomer to the surface will cause hydrophobic recovery. Oxidizing the surface with UV-ozone is an alternative method [14]. Yilgor et al. utilized the method to degrade the methyl groups of silicone-urea materials and a glass-like  $\text{SiO}_x$  surface layer was formed along with some hydrophilic Si–OH groups, resulting in the decrease of hydrophobicity [15]. Unfortunately, this modification may reduce the mechanical properties of silicone hydrogels and cause surface cracking.

In addition, introducing hydrophilic segments or monomers into silicone hydrogels system is a preferable method. One strategy is to blend hydrophilic polymers directly into silicone hydrogels matrix to form an interpenetrating network structure (IPN) [16]. Tang et al. prepared polydimethylsiloxane/2-hydroxyethyl methacrylate (PDMS/PHEMA) silicone hydrogel by means of sequential interpenetrating and found that the incorporation of PHEMA improved the hydrophilicity effectively and reduced the protein adsorption of the material [17]. Mark et al. immobilized hyaluronic acid (HA) in silicone hydrogels and concluded that physical entrapping of HA was beneficial to improve hydrophilicity [18]. Another strategy is to copolymerize or graft hydrophilic polymer segments onto PDMS segments to form block or graft-modified PDMS oligomer, which is then used to copolymerize with hydrophilic monomers to form silicon hydrogels. Lin et al. synthesized the PDMS-PEG copolymer network by chain coupling of hydroxy-terminated PDMS and PEG. The modification resulted in a decrease of the static contact angle from  $105^\circ$  of PDMS to  $20^\circ$  of PDMS-PEG [19]. Yao and Fang added the poly (dimethylsiloxane-ethylene oxide polymeric) (PDMS-*b*-PEO) into the PDMS base and the curing agent to create hydrophilic PDMS-PEO. The contact angle could be controlled between  $21.5$  and  $81^\circ$  according to the change of the mixing ratio [20].

Among these methods, PEG has been explored as a preferred option to copolymerize with silicone monomers and modify the surface of silicone, since PEG is not only non-toxic, biodegradable, biocompatible, and non-antigenic, but also improves the hydrophilicity of silicone hydrogels [21]. Stefanie et al. grafted PEG on PDMS and obtained an amazing decrease of contact angle from  $120^\circ$  of bare PDMS to  $10^\circ$  of PEG-grafted PDMS [22]. Vladkova attached PEG with different molecular weight to silicon rubber surfaces and found that all samples completed  $5$ – $12^\circ$  decrease of contact angle after being immersed into water for  $5$ – $15$  min [23]. Cui et al. reported a synthetic hydrogel synthesized by crosslinking PEG and PDMS and the water content of obtained hydrogels increased with the increase of PEG chains [24]. Moreover, PEG is also a good solubilizer to modify PDMS molecules directly which conveniently increases the intermiscibility of hydrophilic and hydrophobic monomers. Many reports have proved that PEG improves the hydrophilicity of materials. Metha

et al. compared the unmodified chitosan with the ones modified by PEG-PDMS-PEG and found that the water contact angles of the latter ones were smaller [25]. Fatona et al. also reported this method as one-step in mold, and considered it an effective way to render hydrophilicity of PDMS [26].

It is generally known that the composition and length of segments constituting block copolymers have important effects on the properties of the polymers. However, few studies are reported about the effect of chain length of PEG on properties of silicone hydrogels, especially when PEG chains are presented as a segment of PDMS oligomer. In this work, two series of silicone hydrogels based on PEG-PDMS-PEG were prepared, and each series contained  $0$  g/mol,  $200$  g/mol, and  $600$  g/mol PEG chains respectively. The influences of PEG chain length on the hydrophilicity of silicone hydrogels were explored by water contact angle, surface morphology, equilibrium water content, swelling process, dehydration process, and protein adsorption. In addition, the oxygen permeability and the mechanical behavior of silicone hydrogels were also investigated.

## Experimental section

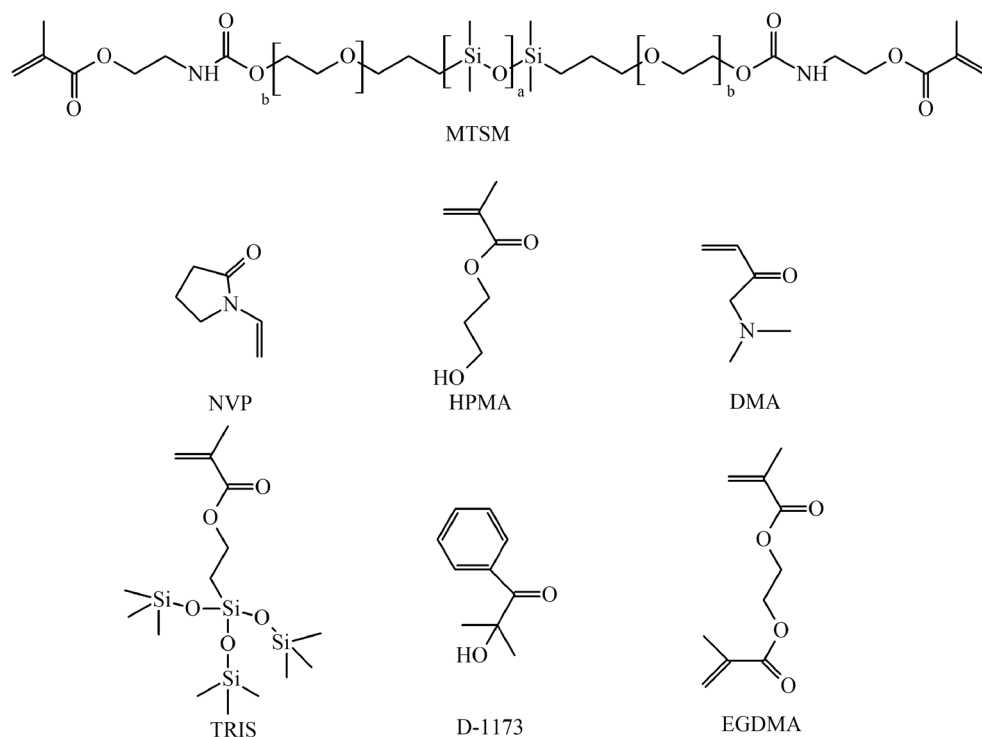
### Materials

Hydroxy-terminated poly (ethylene glycol)–polydimethylsiloxane–poly (ethylene glycol) triblock copolymers (PEG–PDMS–PEG) were supplied by TECH Polymer Copolymer, whose chemical structures were given in Fig. 1 and molecular compositions were listed in Table 1. Isocyanatoethyl methacrylate (IEM) was purchased from Shanghai Ginray Industry. Tris (trimethylsiloxy)-3-methacryloxypropylsilane (TRIS) was bought from TCI. *N,N*-dimethylacetamid (DMA) was acquired from Adamas-beta. *N*-vinyl-2-pyrrolidone (NVP), 2-Hydroxypropyl methacrylate (HPMA), crosslinker ethylene glycol dimethacrylate (EGDMA), photoinitiator darocure1173 (D-1173), and dibutyltin dilaurate (DBTDL) were supplied by Aladdin Chemical Reagent. The isopropyl alcohol (IPA) was purchased from China National Pharmaceutical Group Corporation. The bovine serum albumin (BSA), sodium dodecyl sulfate (SDS), and the bicinchoninic acid (BCA) kits were purchased from Beyotime Biotechnology. All other chemicals were purchased from Sinopharm. All of these materials were used without further purification.

### Preparation of methacrylate-terminated siloxane macromonomer

Based on Peng's [27] method and our preceding study [28], methacrylate-terminated siloxane macromonomer (MTSM) was prepared. PEG-PDMS-PEG and IEM were used and the mole ratio was 1:2. Dichloromethane (DCM) and DBTDL

**Fig. 1** Abbreviations and chemical structures of the monomers, crosslinker, and photoinitiator



were selected as solvent and catalyst respectively. The reactants were mixed and agitated at 35 °C for 24 h for complete reaction, which can be confirmed by the disappearance of the characteristic peak of the isocyanate group ( $-\text{NCO}$ ) at  $2272\text{ cm}^{-1}$  in FTIR spectrum of the solution at the end (24 h) of the reaction. (Figure S1, Supporting Information) Subsequently, the catalyst and the unreacted monomers were removed by petroleum ether extraction and MTSM was gained by evaporating under subatmospheric pressure. The chemical structure of MTSM was given in Fig. 1 and was demonstrated by the appearance of new characteristic peaks of methacrylate group termination ( $\delta = 5.52\text{ ppm}$  (s,  $\text{C}=\text{CH}_2$ ),  $\delta = 6.05\text{ ppm}$  (s,  $\text{C}=\text{CH}_2$ ), ( $\delta = 4.14\text{ ppm}$  (t,  $\text{N}-\text{CH}_2$ )) in the  $^1\text{H-NMR}$  spectra. (Figure S2, Supporting Information) Other monomers, crosslinker, and photoinitiator used in this work were also included in Fig. 1.

**Table 1** Abbreviation and molecular weight of PEG-PDMS-PEG

| Abbreviation | $a$ value <sup>1</sup> | $b$ value <sup>1</sup> | $M_n$ <sup>2</sup> | PDI <sup>2</sup> |
|--------------|------------------------|------------------------|--------------------|------------------|
| 0-1 K-0      | 12                     | 0                      | 1200               | 1.7              |
| 200-1 K-200  | 12                     | 5                      | 1600               | 1.6              |
| 600-1 K-600  | 12                     | 14                     | 2400               | 1.3              |
| 0-4 K-0      | 52                     | 0                      | 3900               | 1.9              |
| 200-4 K-200  | 52                     | 5                      | 4400               | 2.0              |
| 600-4 K-600  | 52                     | 14                     | 5100               | 2.1              |

<sup>1</sup> The values of  $a$  and  $b$  obtained from the manufacturer

<sup>2</sup> The molecular weight of PEG-PDMS-PEG obtained from gel permeation chromatography (GPC) results

## Preparation of silicone hydrogels

The multicomponent silicone hydrogels were manufactured according to our previous work [28]. The silicon-containing monomers (MTSM, TRIS) and hydrophilic monomers (NVP, HPMA, and DMA) were successively added to the beaker, followed by D-1173 as photoinitiator and EGDMA as crosslinking agent. In the two series, the concentrations of D-1173 and EGDMA are constants, both are 0.5 wt%. Lastly, the IPA was added to form a transparent mixed solution. After blending, the mixtures were dripped into the dual-layer polypropylene molds and photopolymerized under 360 nm ultraviolet light at  $13\text{ mW/cm}^2$  for 45 min. After the molds were cooled to room temperature, the copolymer membrane was taken out and washed with ethanol to remove the unreacted monomer and then transferred to distilled water to replace the ethanol. Finally, a transparent silicone hydrogel had been successively prepared. The copolymerization formulations are given in Table 2. The silicone hydrogel samples made from PEG-PDMS-PEG with molecular weights of 0-1 K-0, 200-1 K-200, 600-1 K-600, 0-4 K-0, 200-4 K-200, and 600-4 K-600 are labeled as S(0-1 K-0), S(200-1 K-200), S(600-1 K-600), S(0-4 K-0), S(200-4 K-200), and S(600-4 K-600), respectively.

## Characterization

**Measurement of contact angle** Static water contact angles were measured via the sessile drop method using an optical contact angle goniometer (JY-401). The contact angles were

**Table 2** Copolymerization formulations of silicone hydrogels with different MTSM monomers

| Sample-MW of MTSM | MTSM (mol) | TRIS (mol) | NVP (mol) | HPMA (mol) | DMA (mol) | IPA (mol) | EG unit <sup>1</sup> (mol)% <sup>2</sup> |
|-------------------|------------|------------|-----------|------------|-----------|-----------|--|
| S(0-1 K-0)        | 1.9        | 28.8       | 17.6      | 18.4       | 21.7      | 11.6      | 0.0                                      |
| S(200-1 K-200)    | 1.9        | 28.8       | 17.6      | 18.4       | 21.7      | 11.6      | 14.8                                     |
| S(600-1 K-600)    | 1.9        | 28.8       | 17.6      | 18.4       | 21.7      | 11.6      | 32.7                                     |
| S(0-4 K-0)        | 0.9        | 29.2       | 17.8      | 18.6       | 21.9      | 11.6      | 0.0                                      |
| S(200-4 K-200)    | 0.9        | 29.2       | 17.8      | 18.6       | 21.9      | 11.6      | 6.3                                      |
| S(600-4 K-600)    | 0.9        | 29.2       | 17.8      | 18.6       | 21.9      | 11.6      | 15.8                                     |

<sup>1</sup> EG unit referred to  $-\text{CH}_2\text{CH}_2\text{O}-$ , which was the basic component of PEG

<sup>2</sup> mol% of EG unit =  $\text{MTSM} \times 2 \times b / [\text{MTSM} \times (a + 2b) + \text{TRIS} + \text{NVP} + \text{HPMA} + \text{DMA}]$ . The values of  $a$  and  $b$  in the calculation formula were given in Table 1

tested for a minimum of three identical operations by dropping 5  $\mu\text{L}$  water onto the random position of the sample with a microinjector. The data obtained were expressed as the mean  $\pm$  standard deviation.

**Measurement of surface morphology** The surface morphology was measured by a scanning electron microscopy (SEM, FEI Inspect F50). The samples were cut into strips and then fixed on the sample table with conductive copper glue. Afterwards, the samples were sprayed with gold before being put into the sample chute for testing.

**Measurement of equilibrium water content** The obtained membrane was dried to constant weight in a vacuum oven at 90 °C, and the dry weight  $W_d$  was accurately measured. Then the membrane was immersed in water for 24 h to hydrate sufficiently. The wet weight  $W_s$  was measured after wiping the water on the surface of swollen hydrogels with filter paper. EWC was calculated by Eq. (1).

$$\text{EWC} = \frac{W_s - W_d}{W_s} \times 100\% \quad (1)$$

**Measurement of swelling and dehydration process** The swelling and dehydration performance were measured by weight. For the swelling process, the weights of dry samples were measured as  $W_d$  before they were immersed in water. Then, at regular intervals, the samples were taken out of the water and their weights  $W_t$  were measured after wiping the water on the surface of samples by filter paper. Afterwards, the samples were replaced into the water. The steps were repeated until silicone hydrogels reached equilibrium in the water. The water content (WC) was calculated by Eq. (2).

$$\text{WC} = \frac{W_t - W_d}{W_t} \times 100\% \quad (2)$$

For the dehydration process, the test was carried out in a windless room with a temperature of 23–25 °C, and a relative humidity of 72–75%. The saturated swelling samples were

taken out of the water and wiped by filter paper quickly. The initial water mass was recorded as  $M_{oc}$ . Then, the samples were put into analytical balance. Their weights were recorded to calculate the mass of the lost water called  $M_t$  every once in a while until the value remained unchanged. The dehydration process of silicone hydrogels is shown in Eq. (3). In Eq. (3),  $k^*$  is the constant of dehydration rate and  $n$  is the dynamic series which determines the dehydration mechanism.

$$\frac{M_t}{M_{oc}} = k^*(t)^n \quad (3)$$

**Measurement of protein adsorption** Protein adsorption was determined by a static protein adsorption method with Synergy HT microplate analyzer (Bio-Tek). The BSA solution and SBS solution were prepared with phosphate buffer saline (PBS) solution whose pH was about 7.4. The concentrations of the BSA and SBS solutions were 5 mg/mL and 1 wt% respectively. Silicone hydrogel samples were transferred from the PBS solution to a vial containing 3 mL BSA solution and were incubated at 37 °C for 24 h. After the incubation, the samples were immersed twice in a fresh PBS buffer solution for 30 min each time to wash away the unadsorbed protein. Finally, the samples were transferred to a vial containing 3 mL SDS solution and shaken at 37 °C for 4 h to fully elute the unadsorbed protein, which was the protein solution to be tested. Meanwhile, the BCA working solution was prepared. The BCA solution and the protein solution were dropped into a 96-well plate at a volume ratio of 10:1 and incubated at 60 °C for 30 min to accelerate the color development. The incubated samples were measured with a microplate analyzer by referring the standard curve at 562 nm. Five sets of equilibrium groups were taken for each hydrogel sample.

**Measurement of oxygen permeability coefficient** The oxygen permeability coefficient (Dk) of silicone hydrogels was evaluated by the polarographic method. The oxygen permeation analyzer (Createch 201T Oxygen Permeameter) was used. During the test, the temperature and the moisture content of the

atmosphere should be controlled at  $35 \pm 5$  °C and 95%, respectively. The center thicknesses of samples after fully absorbing water were measured. Then these samples were put on the electrode to get the electric current values. Finally, a function curve of the center thickness-electric current value was made, and the reciprocal of the slope of this curve was the Dk value. The measured values of oxygen permeability were expressed in terms of barrer, which represented the volume of oxygen transmitted. ( $1 \text{ barrer} = 10^{-10} (\text{cm}^3 \times \text{cm})/(\text{cm}^2 \times \text{s} \times \text{cmHg})$ ).

**Measurement of mechanical properties** The mechanical properties of resulting silicone hydrogels were evaluated by using the electronic tensile machine (PC-XLW(L)) with a crosshead speed of 50 mm/min at room temperature. The copolymer membranes were circular shapes with fixed diameter (2 cm) and thickness (0.3 mm).

## Results and discussion

To clarify the influences of molecular weight of PEG on the properties of silicone hydrogels, two series of silicone hydrogels with 1000 g/mol PDMS and 4000 g/mol PDMS respectively were successfully prepared, which could be proved by the existence of characteristic peaks originated from silicon-containing and hydrophilic monomers (Si-CH<sub>3</sub> bending vibration at 1260 cm<sup>-1</sup>, Si-O-Si stretch vibration at 1100 cm<sup>-1</sup>, Si-CH<sub>3</sub> stretching vibration at 800 cm<sup>-1</sup>, C=O stretching vibration at 1720 cm<sup>-1</sup>) and the disappearance of C=C characteristic peak at 1630 cm<sup>-1</sup> in the ATR-FTIR spectrum of the prepared membrane. (Figure S3, Supporting Information). And each series included three different PEG chain length, which were 0 g/mol, 200 g/mol, and 600 g/mol. The silicone hydrogels all have good thermal stability. (Figure S4, Supporting Information). In these multicomponent copolymers, all components were consistent except for siloxane macromolecule MTSM. Furthermore, the effect of the methacrylate terminal groups on the properties of silicone hydrogels can be ignored, because the molecular weight of methacrylate terminal groups is negligible compared with that of the PEG-PDMS-PEG chains. Therefore, the difference of hydrogel properties was mainly attributed to PEG and PDMS segments. The hydrophilicity of silicone hydrogels was characterized by contact angle, equilibrium water content, and swelling-dehydration process, including protein adsorption. The results of oxygen permeability and mechanical properties were also analyzed.

### Water contact angle of silicone hydrogels

The water contact angle is an important parameter to measure the wettability of a material [29]. The images and values of contact angles of silicone hydrogel samples in dry and swollen states were shown in Fig. 2. Two series of silicone hydrogels

showed analogous trends of variation. With the increase of PEG chain length, the water contact angle of the dry samples decreased, while that of the swollen samples increased. Moreover, the difference value between dry and swollen states increased as the chain length of PEG increased. In order to explore the cause for this interesting phenomenon, the surface morphologies of dry samples were characterized.

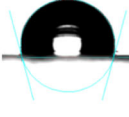
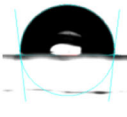
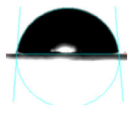
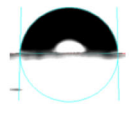
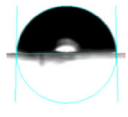
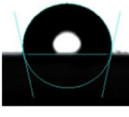
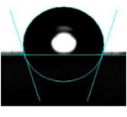
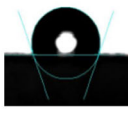
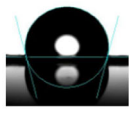
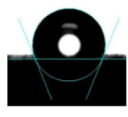
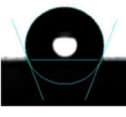
### Surface morphology of silicone hydrogels

The surface morphologies of dry silicone hydrogels were observed by SEM and the results were shown in Fig. 3. Whether the PDMS chains were 1000 g/mol or 4000 g/mol, the variation tendencies of the surface of silicone hydrogel samples were similar. PEG chains can increase the flatness of silicone hydrogels. The silicone hydrogels without PEG chains presented a plicated surface morphology, as shown in Fig. 3(a) and (d). As the PEG chain length increased, the surface of the samples became smoother, as shown in Fig. 3(b) and (e). The effect of PEG chains on silicone hydrogel surface was more obvious when the PEG chain length was 600 g/mol, which presented almost homogeneous and flat surface in Fig. 3(c) and (f). The different surface morphologies of silicone hydrogels with different PEG chain length may be attributable to several factors. Firstly, due to the amphiphathy of PEG chains, the intermiscibility between MTSM with longer PEG chains and hydrophilic monomers was better than the ones with none or shorter PEG chains, which was beneficial to form a homogeneous prepolymer. Secondly, the PEG chains of MTSM interfered with the aggregation of PDMS chains and decreased the size of the silicone phase, and so as decreased the roughness of surface. In addition, during the preparation, some PEG chains occupied surface sites and decreased the silicone content on the surface, which also made contributions to reduce the roughness.

Actually, the surface morphology has a significant influence on the hydrophilicity of materials [30]. With the roughness of the surface increasing, the hydrophilic and hydrophobic membranes will be more hydrophilic and hydrophobic respectively [31]. Since the surfaces of silicone hydrogels were hydrophobic in dry state, the flat surface increased the hydrophilicity. Therefore, the water contact angle of dry samples decreased when the PEG chain length increased.

According to the previous work, if the silicone hydrogels were immersed in water, PEG and PDMS chains would reconstruct over time [32]. In order to explain the reasons for the increase of water contact angle in swollen state, a model of reconstruction was proposed as shown in Fig. 4. Compared with the dry samples, the swollen ones had looser network and the chains stretched further. As shown in Fig. 4(b) and (c), the PEG chains occupied some surface sites in dry states. During the swelling process, the surface reconstruction occurred because of the low surface energy of PDMS chains. The PEG

**Fig. 2** Water contact angle of silicone hydrogels in dry and swollen states

| Sample<br>$\theta$ (°)<br>State | S(0-1K-0)  | S(200-1K-200)  | S(600-1K-600)   | S(0-4K-0)  | S(200-4K-200)  | S(600-4K-600)  |
|---------------------------------|--|--|---|--|--|--|
|                                 | Dry  | <br>$102.0 \pm 1.3$ | <br>$87.2 \pm 2.6$   | <br>$84.9 \pm 1.8$   | <br>$91.7 \pm 1.6$  | <br>$88.4 \pm 1.7$  |
| Swollen                         | <br>$100.8 \pm 2.3$ | <br>$107.1 \pm 1.2$ | <br>$110.4 \pm 0.7$ | <br>$103.6 \pm 2.9$ | <br>$111.8 \pm 0.9$ | <br>$113.2 \pm 1.7$ |

chains on the surface in dry state transferred into the network while the PDMS chains transferred to the surface, as shown in Fig. 4(e) and (f), resulting in a more hydrophobic surface.

Besides, in the formula of these samples, the mole number of every monomer was constant in each series, which meant that the mol% of hydrophilic monomers decreased while the number of EG unit increased in silicone hydrogels which contained long PEG chains. Meanwhile, the hydrophilicity of hydrophilic monomers is better than that of PEG chains, and the longer PEG chains are more flexible and more conducive to the transfer of PDMS chains to the surface. Therefore, the swollen silicone hydrogels with long PEG chains have larger contact angles than the ones with short or none PEG chains.

### Equilibrium water content of silicone hydrogels

The hydrophilicity was also measured by equilibrium water content, and the results were shown in Fig. 5. The trends of the two series were similar. The samples free from PEG chains and containing 600 g/mol PEG had higher water content than

the ones with 200 g/mol PEG. The mole number of every monomer was same in each series of samples. Among these monomers, hydrophilic fraction, including hydrophilic units (EG) and hydrophilic monomers (NVP, HPMA, DMA), contributed greatly to the equilibrium water content. There was a difference in water-absorbing capacity between EG and hydrophilic monomers due to different molecular structure. Besides, MTSM had two methacrylate terminal groups that could act as cross-linkers. Therefore, the crosslinking density of silicone hydrogels decreased along with the PEG chain length increasing. In the two series, NVP, HPMA, DMA were considered as a whole due to the fixed molar ratio and the same changing trend. As shown in Table 2, the mol% of EG increased with the increase of PEG chain length and it could be deduced that the mol% of hydrophilic monomers decreased due to the increasing total mole number. In brief, there was an inverse correlation between the mol% of EG and hydrophilic monomers. Therefore, S(0-1 K-0) and S(0-4 K-0) contained most hydrophilic monomers as the content of EG unit was the least. And these monomers had a great water-absorbing

**Fig. 3** SEM graphs of silicone hydrogels in dry states. **a** S(0-1 K-0), **(b)** S(200-1 K-200), **(c)** S(600-1 K-600), **(d)** S(0-4 k-0), **(e)** S(200-4 K-200), **(f)** S(600-4 K-600)

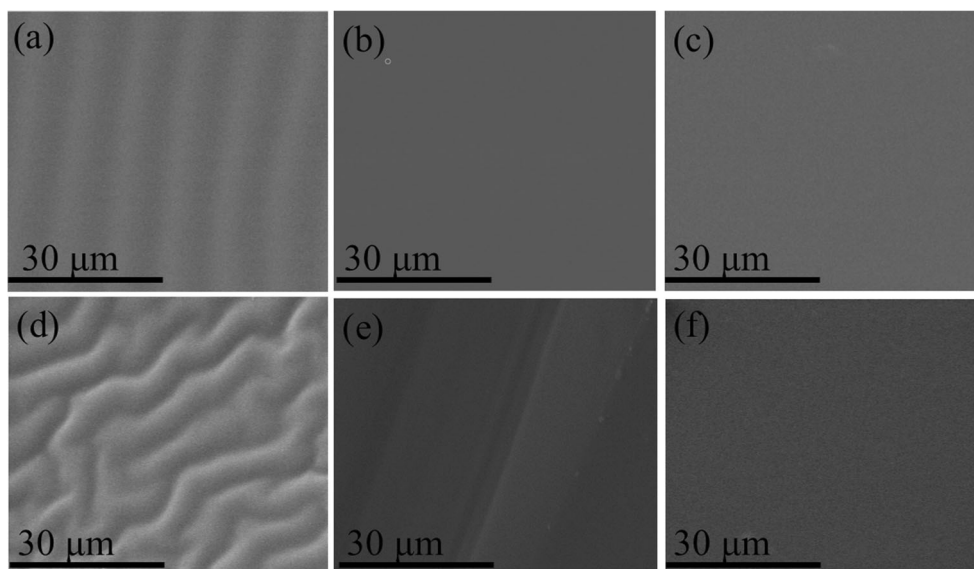
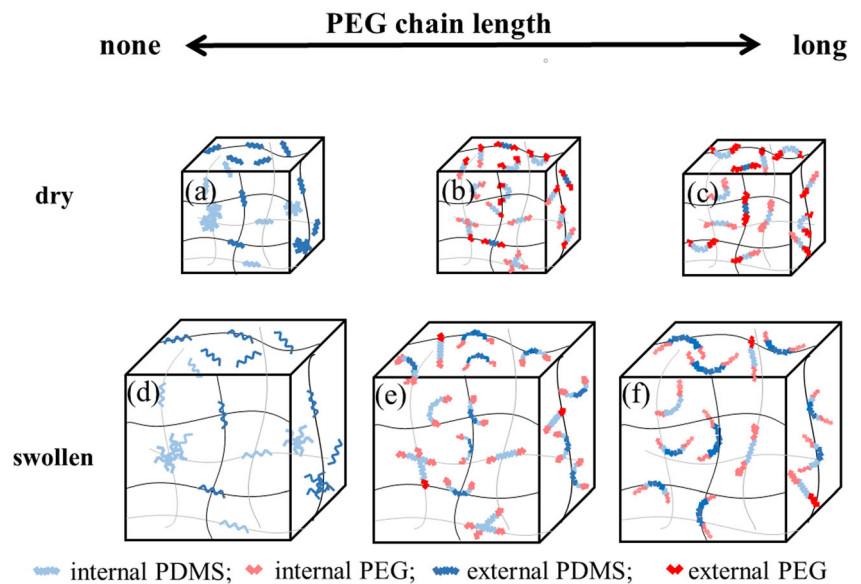


**Fig. 4** A reconstruction model for silicone hydrogels



capacity, which led to higher water content. The hydrophilic monomers of S(200-1 K-200) and S(200-4 K-200) were fewer than that of S(0-1 K-0) and S(0-4 K-0), while they contained 200 g/mol PEG chains. The water-absorbing capacity of short PEG chains is inferior to the ones of reduced hydrophilic monomers, which may lead to a decrease of equilibrium water content. As expected, there was a decrease in each series when the silicone hydrogels contained 200 g/mol PEG chain. S(600-1 K-600) and S(600-4 K-600) had higher water content. This may result from a higher water-absorbing capacity of longer PEG chains and a lower crosslinking density of the network, although the hydrophilic monomers were least corresponding to the highest mol% of EG unit in respective series.

These results showed that PEG chain length, the content of hydrophilic monomers, and crosslinking density in the copolymer synergistically affected the water-absorbing capacity of the silicone hydrogel. In order to study the relationship between PEG chain length and hydrophilicity of silicone hydrogels comprehensively, more details about the swelling and dehydration process were explored.

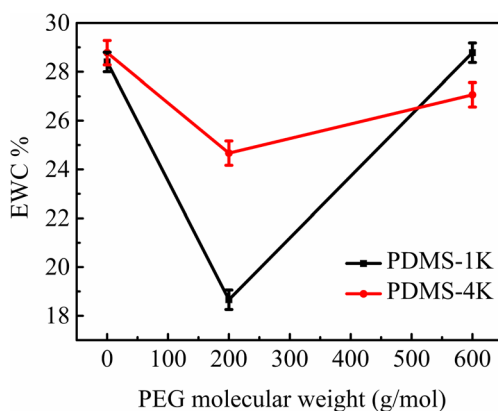


**Fig. 5** Equilibrium water content of silicone hydrogels

### Swelling process of silicone hydrogels

Except for the ultimate water content, the swelling property of silicone hydrogels also changed according to the PEG chain length. The swelling period shortened with the increase of PEG chain length, as shown in Fig. 6. S(0-1 K-0), S(200-1 K-200), and S(600-1 K-600) took 38 min, 21 min, and 16 min to get equilibrium in water respectively. The decreasing trend was similar to the other series whose PDMS chain was 4000 g/mol. S(0-4 K-0), S(200-4 K-200), and S(600-4 K-600) took 120 min, 43 min, and 20 min to get equilibrium in water respectively.

PEG chains made significant contributions to shorten the swelling period of silicone hydrogels. This result was in accordance with that of Zhang's [33]. PEG chains contained a high density of hydroxy, which had strong hydrogen bond interaction with water molecules, resulting in a short swelling period. Longer PEG chains contained more hydroxy and shortened the swelling period further more.

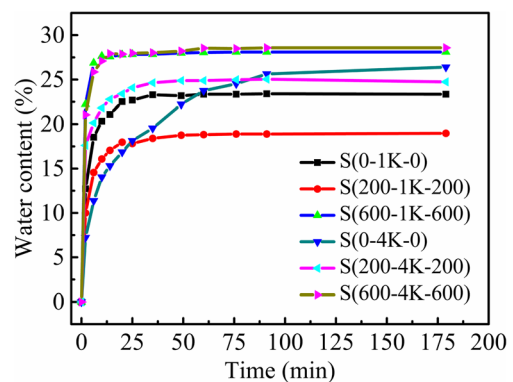


**Fig. 6** Swelling process of silicone hydrogels

## Dehydration process of silicone hydrogels

The series of silicone hydrogels with 1000 g/mol PDMS chains was measured as representative to explore the effect of PEG chain length on dehydration process. The relationship between  $M_t/M_{oc}$  and  $t$  or  $t^{1/2}$  is shown in Fig. 7. It can be seen from Fig. 7(a), during the first period,  $M_t/M_{oc}$  and  $t$  presented a linear relationship, which meant that the dehydration process depended on the evaporation of water on the surface of samples. During this period, the dehydration rate was independent of the equilibrium water content of the hydrogel. S(0-1 K-0), S(200-1 K-200), and S(600-1 K-600) spent 20 min, 22 min, and 24 min for evaporation period respectively. After the water on the surface evaporating completely, the dehydration process turned into the second period, during which  $M_t/M_{oc}$  and  $t^{1/2}$  had a linear relationship, as shown in Fig. 7(b). This period relied on the diffusion of inner water to the surface. The second period lasted longer with the PEG chain length increasing. S(0-1 K-0), S(200-1 K-200), and S(600-1 K-600) spent 10 min, 16 min, and 25 min for diffusion period respectively. Comparing the swelling and dehydration process of silicone hydrogels with different PEG chain length, it was concluded that longer PEG chains gave silicone hydrogels better ability to retain water, which also increased hydrophilicity of silicone hydrogels.

## Protein adsorption of silicone hydrogels

Protein adsorption is an important index of silicone hydrogels especially when used as biomaterials. In this work, the BSA was used as the model protein and the samples with 4000 g/mol PDMS chains were measured as a representative to study the effect of PEG chains on protein adsorption of silicone hydrogels. The results are presented in Fig. 8. Protein adsorption of swollen S(0-4 K-0), S(200-4 K-200), and S(600-4 K-600) were 0.31 mg/cm<sup>2</sup>, 0.16 mg/cm<sup>2</sup>, and 0.23 mg/cm<sup>2</sup> respectively, which indicated that the samples with PEG chains had lower protein adsorption.

Previous studies have shown that PEG segments could inhibit protein adsorptions of materials [34]. Besides, the surface

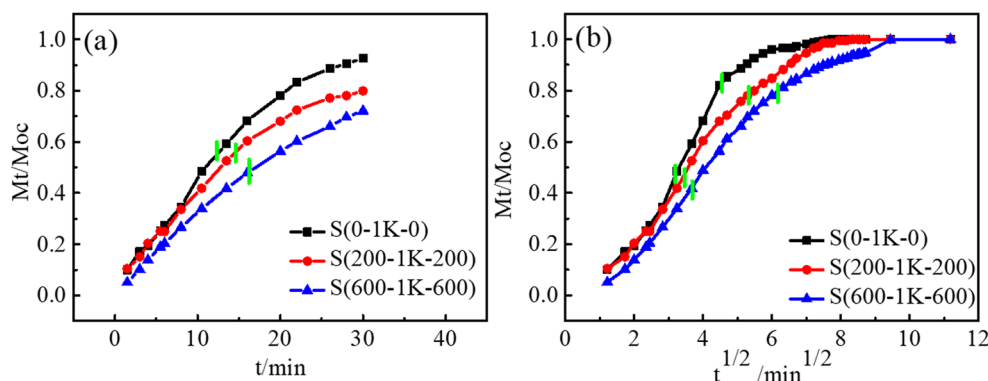
chemical structure and surface morphology of materials also affect the protein adsorption [35, 36]. For the sample S(0-4 K-0), the surface was rough and had no PEG segments, resulting in the highest protein adsorption. According to the SEM results and reconstruction model above, with the increase of PEG chains, the surfaces of silicone hydrogels became smoother and some PEG segments occupied the surface sites, which decreased the protein adsorption. During the surface reconstruction, the longer PEG chains were more flexible, which facilitated the transfer of PDMS segments to the surface, resulting in less PEG segments on the surface of S(600-4 K-600) than that of S(200-4 K-200). Therefore, the surface protein adsorption of S(600-4 K-600) was slightly higher than that of S(200-4 K-200). This result was consistent with that of the contact angle.

## Oxygen permeability of silicone hydrogels

The Dk values of swollen samples are shown in Fig. 9. The silicone hydrogels with 4000 g/mol PDMS had better capability for oxygen transferring than the ones with 1000 g/mol PDMS. Although the siloxane repeat units were of same amount in each series, oxygen permeability presented a decreasing trend as the PEG chain length increased. Because the loose structure of silicone can provide more free volume for the transfer of gas molecules, the silicone component has an extremely high permeability to oxygen [37] and the high oxygen permeability of silicone hydrogels mainly depended on the silicone component. The silicone hydrogels with 4000 g/mol PDMS contained more siloxane repeat units, resulting in higher Dk values.

Due to the poor compatibility between silicon-containing monomers and hydrophilic monomers, microphase separation structures were usually formed in multicomponent silicone hydrogels [38]. The better continuity of silicon phase was more beneficial to oxygen penetration. The PEG chains increased the compatibility of silicon-containing monomers with hydrophilic monomers, which may be hindered the formation of continuous silicon phase and led to the slight decrease of Dk value.

**Fig. 7** Dehydration process of silicone hydrogels





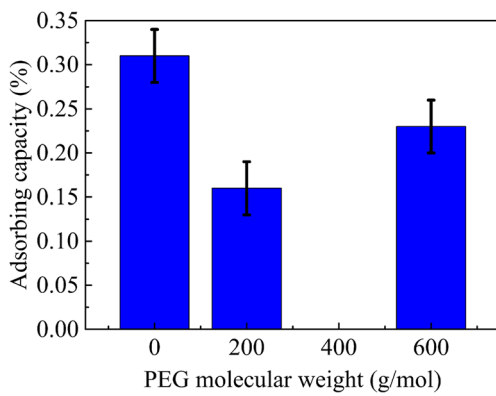


**Fig. 8** The protein adsorption of silicone hydrogels with different PEG chain length

### Mechanical properties of silicone hydrogels

There are several different indicators for evaluating the mechanical properties of a material. The elongation is positively correlated with the tensile properties, so is the tensile strength with the maximum resistance to damage. Meanwhile, the smaller modulus of elasticity reflects the better flexibility of the material. Figure 10 showed the relationship of PEG chain length with elongation, modulus, and tensile strength of silicone hydrogels. Both series of silicone hydrogels presented a decreasing trend of mechanical properties with the increase of PEG chain length.

In the previous work, PEG chains can improve the mechanical properties of materials if they form crystalline region in silicone hydrogels [39]. However, no crystalline region is found in these samples, so PEG chains are also “soft part” of the material, resulting in the decrease of the hardness of silicone hydrogels. Therefore, the moduli of silicone hydrogels decreased when the PEG chain became longer. Moreover, with the increase of PEG chain length, the crosslinking density of samples decreased, and this maybe the other reason for the decrease of elongation and tensile strength.

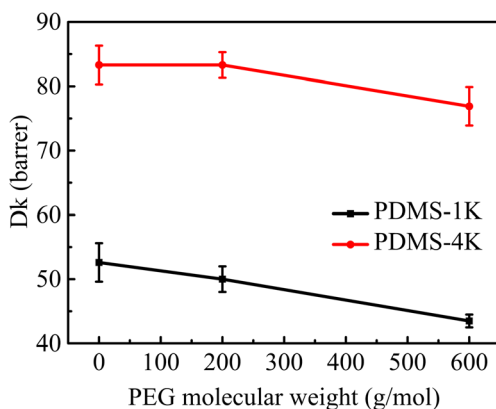


**Fig. 9** Oxygen permeability of silicone hydrogels in swollen state

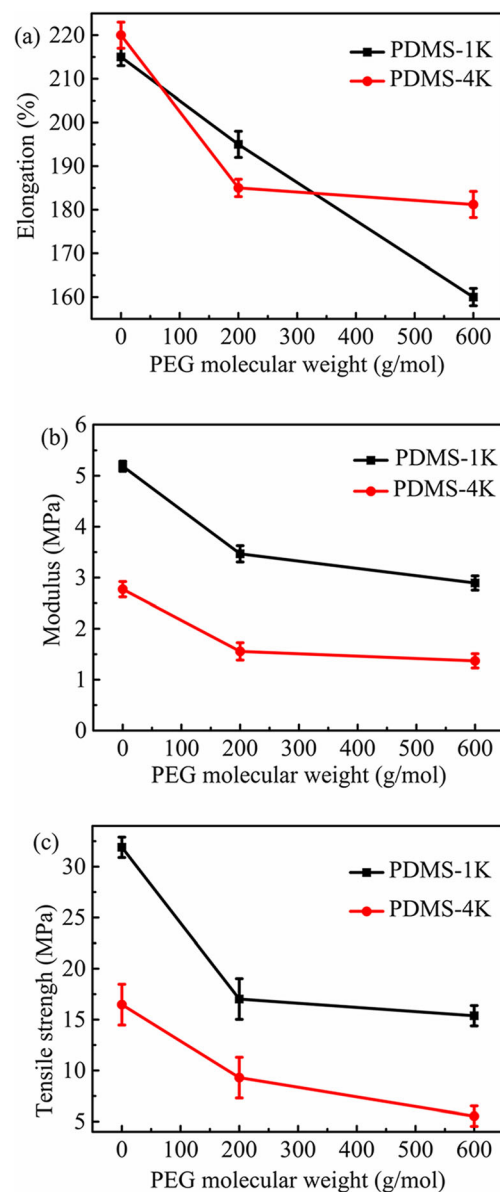


**Fig. 10** a Elongation, (b) modulus, and (c) tensile strength of silicone hydrogels in swollen state

### Conclusions

Two series of silicone hydrogels containing different PEG chain length were synthesized through copolymerization of silicon-containing and hydrophilic monomers. As the PEG segment increased, water contact angles of dry samples presented a decreasing trend while the ones of swollen samples presented an increasing trend. The surface morphology showed that the flatness of surface increased with the PEG chain length increasing. The increasing flatness of surface and wettable PEG segment resulted in the decrease of contact angle in the dry state. A reconstruction model of swollen samples was proposed, and explained that PDMS and PEG chains reconstructed during the swelling process, resulting in a hydrophobic recovery of

surface and the increasing water contact angle of swollen samples. The equilibrium water content of silicone hydrogels depended on the synergy of PEG chain length, hydrophilic monomer content, and crosslinking density in the copolymer. The samples with 600 g/mol PEG chains had higher water content. Swelling and dehydration process indicated that longer PEG chain length improved the water-absorbing ability of silicone hydrogels. PEG chains inhibited the protein adsorption because the surfaces of silicone hydrogels became smoother and some PEG segments occupied surface sites. The oxygen permeability presented a slight decrease as the PEG chain length increased. In addition, the mechanical properties of silicone hydrogels decreased due to the soft PEG chains.

**Funding information** This work was financially supported by the Natural Science Foundation of Jiangsu Province (BK20130617, BK20130619), the National Natural Science Foundation of China (Grant No. 21374016, 21304018), and the Priority Academic Program Development of Jiangsu Higher Education Institutions.

### Compliance with ethical standards

**Conflict of interest** The authors declare that they have no conflicts of interest.

### References

1. Tighe BJ (2013) A decade of silicone hydrogel development: surface properties, mechanical properties, and ocular compatibility. *Eye Contact Lens* 39(1):4–12
2. Sugimoto H, Nishino G, Tsuzuki N, Daimatsu K, Inomata K, Nakanishi E (2012) Preparation of high oxygen permeable transparent hybrid copolymers with silicone macro-monomers. *Colloid Polym Sci* 290(2):173–181
3. Nicolson PC, Vogt J (2001) Soft contact lens polymers: an evolution. *Biomaterials* 22(24):3273–3283
4. Caló E, Khutoryanskiy VV, Reading TUo (2015) Biomedical applications of hydrogels: a review of patents and commercial products. *Eur Polym J* 65:252–267
5. Morales-Hurtado M, Zeng X, Gonzalez-Rodriguez P, Elshof JET, Heide EVD (2015) A new water absorbable mechanical epidermal skin equivalent: the combination of hydrophobic PDMS and hydrophilic PVA hydrogel. *J Mech Behav Biomed Mater* 46:305–317
6. Hamid ZAA, Lim KW (2016) Evaluation of UV-crosslinked poly (ethylene glycol) diacrylate/poly (dimethylsiloxane) dimethacrylate hydrogel: properties for tissue engineering application. *Proc Chem* 19:410–418
7. Xu J, Li X, Sun F (2011) In vitro and in vivo evaluation of ketotifen fumarate-loaded silicone hydrogel contact lenses for ocular drug delivery. *Drug Deliv* 18(2):150–158
8. Wang J, Fang L, Wei J (2012) Hydrophilic silicone hydrogels with interpenetrating network structure for extended delivery of ophthalmic drugs. *Polym Adv Technol* 23(9):1258–1263
9. Rudy A, Kuliasha C, Uruena J, Rex J, Schulze KD, Stewart D, Angelini T, Sawyer WG, Perry SS (2017) Lubricous hydrogel surface coatings on polydimethylsiloxane (PDMS). *Tribol Lett* 65(1):3
10. Oláh A, Hillborg H, Vancso GJ (2005) Hydrophobic recovery of UV/ozone treated poly (dimethylsiloxane): adhesion studies by contact mechanics and mechanism of surface modification. *Appl Surf Sci* 239(3):410–423
11. David T, Puccinelli JP, Beebe DJ (2006) Thermal aging and reduced hydrophobic recovery of polydimethylsiloxane. *Sensors Actuators B Chem* 114(1):170–172
12. Vlachopoulou ME, Petrou PS, Kakabakos SE, Tseripi A, Beltsios K, Gogolides E (2009) Effect of surface nanostructuring of PDMS on wetting properties, hydrophobic recovery and protein adsorption. *Microelectron Eng* 86(4):1321–1324
13. Bhattacharya S, Datta A, Berg JM, Gangopadhyay S (2005) Studies on surface wettability of poly (dimethyl) siloxane (PDMS) and glass under oxygen-plasma treatment and correlation with bond strength. *J Microelectromech Syst* 14(3):590–597
14. Kun M, Javier R, Hirasaki GJ, Sibani Lisa B (2011) Wettability control and patterning of PDMS using UV-ozone and water immersion. *J Colloid Interface Sci* 363(1):371–378
15. Yilgor E, Kaymakci O, Isik M, Bilgin S, Yilgor I (2012) Effect of UV/ozone irradiation on the surface properties of electrospun webs and films prepared from polydimethylsiloxane–urea copolymers. *Appl Surf Sci* 258(10):4246–4253
16. Charles W, Schmidt G, Wilker JJ (2013) A review on tough and sticky hydrogels. *Colloid Polym Sci* 291(9):2031–2047
17. Tang Q, Yu JR, Chen L, Zhu J, Hu ZM (2011) Poly (dimethyl siloxane)/poly (2-hydroxyethyl methacrylate) interpenetrating polymer network beads as potential capsules for biomedical use. *Curr Appl Phys* 11(3):945–950
18. Mark VB, Andrea W, Lyndon J, Heather S (2008) Immobilized hyaluronic acid containing model silicone hydrogels reduce protein adsorption. *J Biomater Sci Polym Ed* 19(11):1425–1436
19. Lin G, Zhang X, Kumar SR, Mark JE (2010) Modification of polysiloxane networks for biocompatibility. *Mol Cryst Liq Cryst* 521(1):56–71
20. Yao M, Ji F (2012) Hydrophilic PEO-PDMS for microfluidic applications. *J Micromech Microeng* 22(2):025012
21. Garay RP, Raafat EG, Armstrong JK, George G, Pascal R (2012) Antibodies against polyethylene glycol in healthy subjects and in patients treated with PEG-conjugated agents. *Exp Opin Drug Deliv* 9(11):1319–1323
22. Demming S, Lesche C, Schmolke H, Klages CP, Büttgenbach S (2011) Characterization of long-term stability of hydrophilized PEG-grafted PDMS within different media for biotechnological and pharmaceutical applications. *Phys Status Solidi* 208(6):1301–1307
23. Vladkova T (2010) Surface modification of silicone rubber with poly (ethylene glycol) hydrogel coatings. *J Appl Polym Sci* 92(3): 1486–1492
24. Cui J, Lackey MA, Tew GN, Crosby AJ (2012) Mechanical properties of end-linked PEG/PDMS hydrogels. *Macromolecules* 45(15):6104–6110
25. Rutnakornpituk M, Ngamdee P, Phinyocheep P (2006) Preparation and properties of polydimethylsiloxane-modified chitosan. *Carbohydr Polym* 63(2):229–237
26. Fatona A, Chen Y, Reid M, Brook MA, Moran-Mirabal JM (2015) One-step in-mould modification of PDMS surfaces and its application in the fabrication of self-driven microfluidic channels. *Lab Chip* 15(22):4322–4330. <https://doi.org/10.1039/c5lc00741k>
27. Peng S, Guo Q, Hughes TC, Hartley PG (2011) In Situ Synchrotron SAXS study of Polymerizable microemulsions. *Macromolecules* 44(8):3007–3015. <https://doi.org/10.1021/ma102978u>
28. Tao H, Zhang X, Sun Y, Yang H, Lin B (2016) The influence of molecular weight of siloxane macromere on phase separation morphology, oxygen permeability, and mechanical properties in multi-component silicone hydrogels. *Colloid Polym Sci* 295(1):205–213. <https://doi.org/10.1007/s00396-016-4001-9>

29. Maldonado-Codina C, Morgan PB (2007) In vitro water wettability of silicone hydrogel contact lenses determined using the sessile drop and captive bubble techniques. *J Biomed Mater Res A* 83(2):496–502. <https://doi.org/10.1002/jbm.a.31260>
30. Maghsoudy-Louyeh S, Ju HS (2010) Tittmann BR surface roughness study in relation with hydrophilicity/hydrophobicity of materials using atomic force microscopy
31. Shirtcliffe NJ, Mchale G, Atherton S, Newton MI (2010) An introduction to superhydrophobicity. *Adv Colloid Interf Sci* 161(1):124–138
32. Sundaram HS, Cho Y, Dimitriou MD, Weinman CJ, Finlay JA, Cone G, Callow ME, Callow JA, Kramer EJ, Ober CK (2011) Fluorine-free mixed amphiphilic polymers based on PDMS and PEG side chains for fouling release applications. *Biofouling* 27(6):589–602. <https://doi.org/10.1080/08927014.2011.587662>
33. Zhang Y, Lin Y (2011) Improvement of permeability of poly (vinyl alcohol) hydrogel by using poly (ethylene glycol) as Porogen. *J Macromol Sci D Rev Polym Process* 50(8):776–782
34. Xiaole MA, Yanlei SU, Qiang S, Wang Y, Jiang Z (2007) Preparation of protein-adsorption-resistant polyethersulfone ultrafiltration membranes through surface segregation of amphiphilic comb copolymer. *J Membr Sci* 292(1):116–124
35. Olanya G, Thormann E, Varga I, Makuska R, Claesson PM (2010) Protein interactions with bottle-brush polymer layers: effect of side chain and charge density ratio probed by QCM-D and AFM. *J Colloid Interface Sci* 349(1):265–274. <https://doi.org/10.1016/j.jcis.2010.05.061>
36. Latour RA (2005) Biomaterials: protein–surface interactions
37. Berean K, Ou JZ, Nour M, Latham K, McSweeney C, Paull D, Halim A, Kentish S, Doherty CM, Hill AJ, Kalantar-zadeh K (2014) The effect of crosslinking temperature on the permeability of PDMS membranes: evidence of extraordinary CO<sub>2</sub> and CH<sub>4</sub> gas permeation. *Sep Purif Technol* 122:96–104. <https://doi.org/10.1016/j.seppur.2013.11.006>
38. Zhao Z, Xie H, An S, Jiang Y (2014) The relationship between oxygen permeability and phase separation morphology of the multicomponent silicone hydrogels. *J Phys Chem B* 118(50):14640–14647. <https://doi.org/10.1021/jp507682k>
39. Sun G, Zhang XZ, Chu CC (2008) Effect of the molecular weight of polyethylene glycol (PEG) on the properties of chitosan-PEG-poly(N-isopropylacrylamide) hydrogels. *J Mater Sci Mater Med* 19(8):2865–2872. <https://doi.org/10.1007/s10856-008-3410-9>

**Publisher's note** Springer Nature remains neutral with regard to jurisdictional claims in published maps and institutional affiliations.